Faraday Discussions

Accepted Manuscript

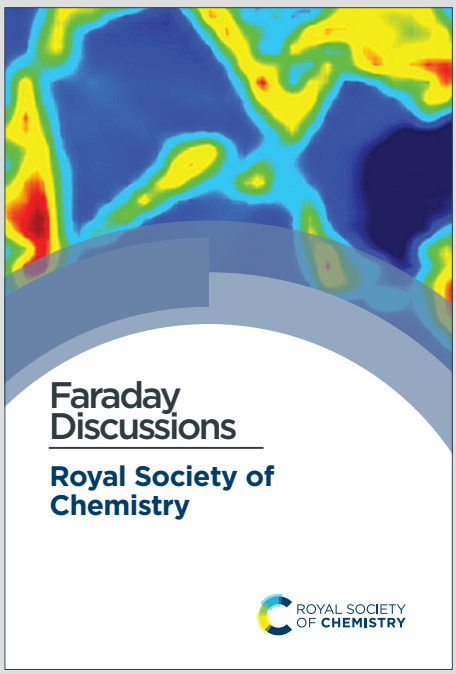

This article can be cited before page numbers have been issued, to do this please use: A. Molle, G. Faraone, A. Lamperti, D. Chiappe, E. Cinquanta, C. Martella, . E. Bonera , E. Scalise and C. Grazianetti, *Faraday Discuss.*, 2020, DOI: 10.1039/C9FD00121B.

View Article Online
DOI: 10.1039/C9FD00121B

PAPER

Stability and universal encapsulation of epitaxial Xenes

Alessandro Molle,*[a] Gabriele Faraone,[a,b] Alessio Lamperti,[a] Daniele Chiappe,[a,†] Eugenio Cinquanta,[c] Christian Martella,[a] Emiliano Bonera,[b] Emilio Scalise,[b] and Carlo Grazianetti[a]

Received 00th January 20xx,
Accepted 00th January 20xx

DOI: 10.1039/x0xx00000x

In the realm of two-dimensional materials framework, single-element graphene-like lattices, known as Xenes, pose several issues concerning their environmental stability with implication in their use for technology transfer to a device layout. In this Discussion, we scrutinize the chemical reactivity of epitaxial silicene, taken as a case in point, in oxygen-rich environments. Oxidation of silicene is detailed by means of a photoemission spectroscopy study upon carefully dosing molecular oxygen in vacuum and subsequent exposure to ambient conditions, showing different chemical reactivity. We therefore propose a sequential Al_2O_3 encapsulation of silicene as a solution to face degradation proving effectiveness by virtue of the interaction between silicene and silver substrate. Based on this direction, we generalize our encapsulation scheme to a large number of metal-suported Xenes by taking the case of epitaxial phosphorene-on-gold into account.

Introduction

Epitaxial Xenes are a quickly emerging reality in the realm of two-dimensional (2D) crystals beyond graphene. They were recently sorted in two generations according to the position of the constitutive element (X) in the periodic table (first generation including elements of the silicon group, whereas the second one gathers elements of boron, nitrogen, and oxygen groups.[1] Compared to other 2D players, they constitute a broad portfolio of materials with variable and configurable properties depending on the growth environment (e.g. the substrate) or the atomistic details (e.g. the buckled bonding). As epitaxial materials, they are scalable thus looking promising for industrial applications. The heavier amid them are also prone to host a 2D topological insulating state of matter.[2,3] While structure and electronic properties may vary throughout the Xenes generations,[4,5] a common issue for all single-layer Xenes relies on the stability against environmental reactivity. This is basically due to the fact that bonding in Xenes are less stable than in graphene or other layered compounds. A paradigmatic example in this respect is silicene (and silicene-like materials like germanene and stanene) where pseudo sp^2 bondings are artificially induced by means of configurational constraints.[6] This synthetic set-up poses several questions concerning the stability of silicene and akin materials. For instance, is silicene prone to degradation under ambient condition? How does silicene undergo oxidation? How to protect silicene from degradation? And how to extend such a protective process to the whole class of Xenes? All along this line, in this Discussion, we elaborate on specific aspects of the chemical stability of the Xenes by reporting on original data about the exposure of epitaxial silicene to O_2-rich ambient in ultra-high vacuum (UHV) growth condition. Silicene as well as other Xenes turn out to undergo degradation in environmental conditions unless a protective layer is applied. Encapsulation, as opposed to passivation, aims at forming a barrier to the external atmosphere without changing neither the bonding nor the functional properties of the Xenes. This can be a difficult task because we need the encapsulating layer to grow on top of the Xene, while having a minimum interaction with it**.** In this respect, we state the condition for a universal encapsulation scheme for metal-supported Xenes and support it with a preliminary *ab initio* model. To corroborate the universal character of the approach, we scrutinize the epitaxial phosphorene on Au(111) as a second case in point.

Silicene reactivity

Oxidation of silicon constituted a milestone in integrated microelectronic circuits enabling the ubiquitous integration of silicon. Now that silicon-based devices are approaching ultimate scaling, oxidation of silicene, namely silicon at the 2D level, may open new technology paths of silicon exploitation in nanoelectronics. One way in this direction is to investigate how the chemical bonding in the epitaxial silicene is affected by an oxygen-rich environment. We elucidate this scenario in variable dosage experiment starting from an UHV condition and by

[a] *CNR-IMM, unit of Agrate Brianza, via C. Olivetti 2, 20864 Agrate Brianza (Italy).*
[b] *Dipartimento di Scienza dei MaterialiUniversità degli Studi Milano-Bicocca, via R. Cozzi 55, 20125, Milano, Italy).*
[c] *CNR-IFN, Piazza Leonardo da Vinci 32, 20133 Milano (Italy)*
† Present address: ASM Microchemistry, Pietari Kalmin katu 3, 00560 Helsinki (FI)
Electronic Supplementary Information (ESI) available: [details of any supplementary information available should be included here]. See DOI: 10.1039/x0xx00000x

monitoring the synchrotron radiation Si 2*p* core-level photoemission line of epitaxial silicene-on-silver(111) with increasing O_2 partial dose. Two silicene configurations were taken into account, the low-temperature mixed 4x4/√13x√13 phase (**Figure 1a**) and the high-temperature 2√3x2√3 phase (**Figure 1b**) as they were proven to be the precursors for room temperature operational field effect transistor.[7] Basically, the two configurations differ in terms of their buckled bond pattern,[8] as markedly evidenced by the different positioning of the E_{2g} Raman mode as well as lower frequency features.[9] For each configuration, Si 2*p* spectra are reported for the freshly grown silicene, after 75 L and 750 L O_2 exposure. The Si 2*p* line of the freshly grown silicene phases displays a multipeak shape profile that was previously rationalized as coming from the interplay of three different elemental (Si-Si) bonding environments termed Si^{α}, Si^{β}, and Si^{γ}.[10] Similar to Fleurence et al.,[11] these components reflect different positioning of the Si atoms with respect to the Ag surface, namely hollow sites, intermediate sites, and coincidence sites. This substrate sensitivity was also observed in a position-dependent local density of states.[12] Limited oxidation takes place with varying the O_2 dosage from 75 to 750 L as one may deduce from the emergence of a minor feature at that is characteristic of Si^{4+} bonding in SiO_2 (see also the magnification of the spectral region in the insets). Conversely, the Si 2*p* profile dramatically changes in the proportion of its elemental components. This fact is apparent from the evolution of the Si 2*p* line as a function of the O_2 dosage in both silicene configurations. This aspect relies on a substantial variation of the bonding population inside each individual silicene phase as a consequence of the oxygen exposure. In other words, silicene reacts against O_2 exposure by rebalancing its elemental bonding components with respect to its pristine form while SiO_2 bonding formation is quite limited. In detail, the Si^{α} component corresponding to hollow sites of silicon atoms undergoes a relative increase with increasing the O_2 exposure from 75 to 750 L. Qualitatively, this behaviour looks like a silicene lattice rearrangement with silicon atoms preferentially positioning far from underlying Ag atoms as if this recombination could diminish the interaction of silicene with the substrate. This picture can be related to previously reported O_2 intercalation in silicon bilayer.[13] If so, an *open question* is how post-growth O_2 exposure can be exploited to disentangle silicene from its substrate without corrupting its elemental lattice and with a substantial benefit in transfer of silicene into a device substrate.[7]

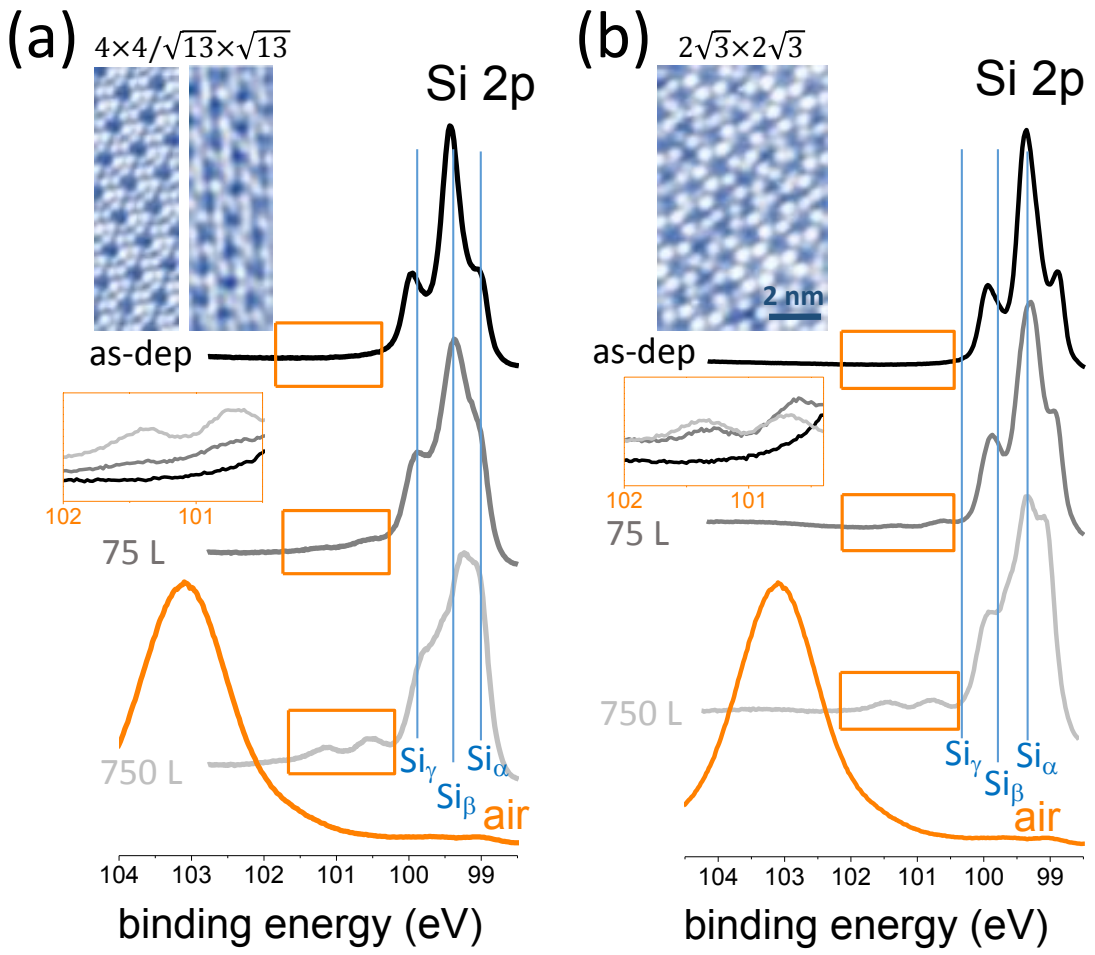

Figure 1 Si 2*p* core level photoemission lines (from top to bottom) for freshly grown silicene-on-silver, after 75 L O_2 exposure, after 750 L O_2 exposure, and after exposure to air. Core level lines are reported for two different silicene configurations, the mixed phase 4x4/√13x√13 (a) and the 2√3x2√3 phase (b). Images at the top of each panel are scanning

tunneling topographies of the two configurations. Insets in both panels (intermediate position at left side of the panels) are magnifications of a limited range of the Si 2*p* lines in order to elucidate O_2-induced oxidation of silicene.

View Article Online
DOI: 10.1039/C9FD00121B

Ultimately, if silicene is exposed to air, complete oxidation in a SiO_2 compound takes place as follows from the emergence of a broad peak at 103.50 eV corresponding to the Si^{4+} valence state in Si bonding. In this latter stage, it is not clear at the moment whether this silicene-derived SiO_2 recasts as a 2D oxide layer (conformal to the original silicene) or as a clustered adsorbate. *Open questions* remain as to what kind of oxidation may take place when considering multilayer silicene as long as this configuration represents an alternative to conventional cubic-structured silicon where to unravel new mechanism for silicon oxidation. More specifically, we wonder whether silicene can be uniformly oxidized so as to form a 2D silicon oxide either in the single layer or in multilayer state. If so, we also wonder to what extent this silicene oxide would differ from 2D silicon oxide frameworks grown on metal surfaces as reported by Buchner et al.[14] This is an interesting bunch of questions aiming at the development of a new fashion of 2D insulators.

Encapsulation of silicene

The experimental framework

Environmental oxidation of silicene is a hurdle for usage in applications. Methods to save silicene from degradation were demanding since the early stages of the silicene debut. One possible effective option turned out to be the Al_2O_3 encapsulation sequentially carried out in UHV condition after silicene growth by means of reactive co-deposition of an atomic Al beam with O2 molecules.[15] This methodology results in the preservation of the chemical environment of silicene by means of a protective Al_2O_3 layer on silicene by sequentially growing an elemental Al in a first stage, and Al in O_2 rich environment in a second stage. The initial elemental Al prevents silicon from oxidation when inletting the O_2 gas in the second stage so as to have an overall Al_2O_3 layer in the end. No chemical interaction occurs between silicene and Al_2O_3 as demonstrated by the unaltered shape profile of the Si 2*p* core level photoemission line in **Figure 2a** prior to and after Al_2O_3 deposition. Extra Ag 4*s* feature from substrate in the Si 2*p* line of the pristine silicene does not appear after encapsulation owing to the added Al_2O_3 thickness and accordingly reduced substrate sensitivity in the photoemission. The Al_2O_3 encapsulation presents several benefits. It is a sequential process with the silicene epitaxy within the same UHV ambient. As such, it is not affected by collateral contamination. It works as an insulating layer for all those applications where a gate is needed. The effectiveness of the Al_2O_3 encapsulation is phenomenological evidence substantiated by in situ X-ray photoelectron spectroscopy (XPS) and ex situ Raman spectroscopy as reported in **Figure 2**.

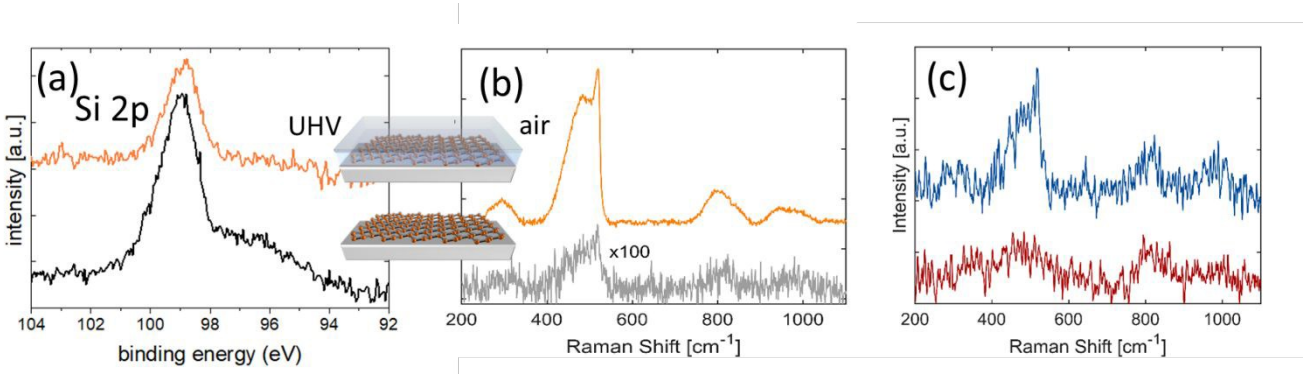

Figure 2 (a) Si 2p core-level photoemission lines taken on a freshly grown silicene-on-silver (bottom) and after Al_2O_3 encapsulation (top). The right-side feature in the former spectrum is related to Ag 4s photoemission from substrate, no longer detected in the encapsulated silicene owing to the Al_2O_3 layer thickness (~5 nm); (b) Raman spectra of (top) capped and (bottom) uncapped Silicene/Ag(111), in both cases the samples are exposed to air when recording the Raman spectrum and the silicene lattice is preserved only in case of the encapsulated sample; (c) Raman spectra of unprotected Silicene/Ag(111) obtained 1 minute (top same as bottom spectrum in panel b) and □5 minutes after the air exposure (bottom). The spectra are vertically stacked for clarity.

As an identification probe, Raman spectroscopy proved to be a superior tool to identify graphene and graphene-related materials, generally.[16] It was used for silicene too in order to check the silicene integrity after encapsulation as reported in **Figure 2a**. This is demonstrated in the comparative Raman spectroscopy study in **Figure 2b**. In detail, **Figure 2b** compares the encapsulated silicene (in air) with uncapped silicene in the early stage of degradation upon exposure to ambient air. The spectrum of silicene-on-silver(111) acquired just after its exposure to ambient conditions, shows a feature around 500 cm^{-1}, composed by a prominent narrow peak at 516 cm^{-1} plus a broad shoulder on the lower energy side (□460 cm^{-1}). These features are compatible with the Raman active modes of silicene-on-silver(111) substrates maintained in UHV conditions[17] and, together with the band at 800 cm^{-1}, are indicative of the presence of a partially oxidized ordered SiO_2 phase.[18] More detailed characterization of the Raman spectrum of silicene is extensively reported elsewhere.[9] What matters here is to emphasize the effectiveness of the encapsulation in preserving silicene from degradation when directly exposed. Nonetheless, fast degradation occurs as follows from the XPS spectra reported in **Figure 1** for both silicene layouts after exposure to air. The dynamics of silicene oxidation is so fast that a close real-time monitoring of silicene evolution is necessary to unveil the mechanism of the Si reactivity under environmental condition.

View Article Online
DOI: 10.1039/C9FD00121B

As uncapped silicene is extracted from the growth chamber and brought to ambient conditions, the reaction with O_2 immediately occur, as evidenced by the Raman spectrum reported in **Figure 2c**. Sizable modifications affect the Raman spectrum as a function of the exposure time. The disappear of the sharp peak is accompanied by the broadening of the feature at 500 cm^{-1}, whose intensity becomes comparable with the feature at 800 cm^{-1}. These two observations may reflect the complete amorphization of the SiO_2 phase resulted from the early exposure thus confirming recent result obtained by means of in situ Raman spectroscopy at low O_2 dose.[19] The dynamics of the bare silicene/Ag(111) exposed to ambient conditions is clearly dominated by the reaction with O_2. The overall process could be depicted as a two-step reaction. The early interaction of the silicene layer with O_2 leads to the formation of a partially ordered SiO_2 phase clusters with a small portion of silicene in its original structure. As the process progresses, the system evolves towards the amorphous phase of the thin cluster-assembled SiO_x. To confirm this two-step picture and finely describe the silicene degradation process, an in situ monitoring of the structural properties of the system as a function of the O_2 dose would help to disentangle the two proposed kinetics. The initial tendency of the silicene layer to preserve its order may be related to the interaction with the metallic substrate that makes Si atoms to be less prone to oxidation. Overall, *a question arises on what mechanism favours Al_2O_3 to accommodate on silicene-on-Ag without apparently affecting its structure*.

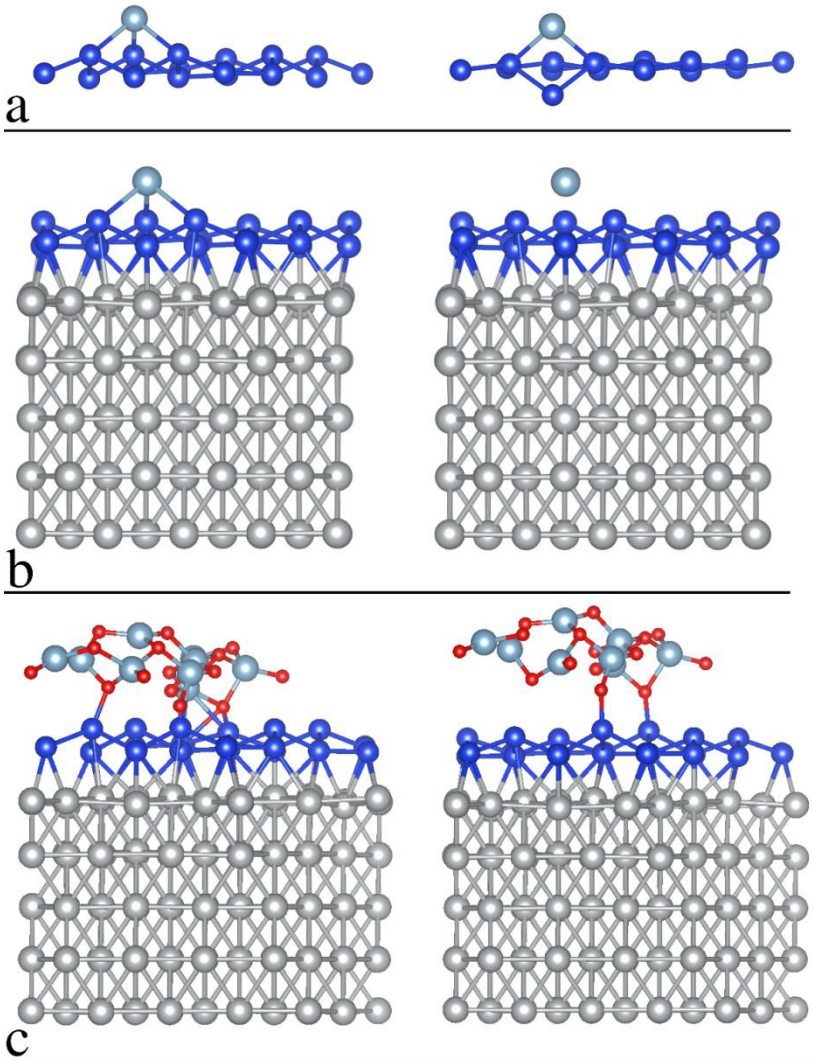

Figure 3 DFT simulation before relaxation (left) and after relaxation (right) in case of: a) Al atom absorption to free-standing silicene, b) Al atom absorption to silicene-on-silver, c) Al_2O_3 accommodation on silicene-on-silver.

A theoretical framework

An argument to support this picture comes from preliminary density functional theory (DFT) simulations of silicene reactivity towards Al atom adsorption first, and Al_2O_3 accommodation secondly. We propose simulations for two different configurations, free-standing silicene and a silicene-on-Ag. In order to further investigate this mechanism, a preliminary *ab initio* investigation on the interaction between Al or O_2 and a 4x4 reconstruction of silicene on Ag(111) has been performed by means of DFT calculations detailed in the method section. Results of the structural relaxations are summarized in **Figure 3** where two relevant aspects can be highlighted. First, an Al atom (light blue spheres) turns out to be favorably incorporated in the crystal lattice of free-standing silicene and it strongly affects the silicene structure (blue sphere lattice) after relaxation (**Figure 3a**) whereas the same atom on the Ag-supported silicene (**Figure 3b**, bottom scheme) tends to move apart

from the Si surface upon relaxation. Hence, one can infer that the silicene layer is chemically "protected" by the hybridization of the Si atoms with Ag atoms of the substrate, and in fact the calculated binding energy of the Al atom on the silicene layer is reduced by about 0.25 eV in presence of the Ag substrate, as compared to the free-standing case. It should be noticed that this is a tendential behavior for an individual Al adatom accommodating on the silicene face that can be hardly matched with a collective behavior of an Al layer grown on silicene. Nonetheless, this individual picture gives us an idea on the tendential influence of the Ag substrate on the silicene reactivity during Al_2O_3 deposition. In the latter case, the "lower reactivity" of the Ag-supported silicene (compared to the free-standing case) leads the O_2 molecule (O atoms are pictured as red spheres in **Figure 3**) to preferably bind with Al atoms, resulting in a relaxed structure that only marginally influences the silicene bonds (see **Figure 3c**) illustrating the as grown and the relaxed Al_2O_3 on Ag-supported silicene). It should be noticed that this picture is only specific of the Ag-supported silicene, but it may fail in other cases, e.g. silicene on ZrB_2 where the extent of the hybridization between the silicene layer and the substrate can change. Although it was noticed that an effective encapsulation can be substrate-dependent,[20] this preliminary outcome suggests a direction to apply the Al_2O_3 encapsulation to Xenes supported by noble metal surfaces.

Though preliminary, these data shows that the Al_2O_3 capping protocol can be applied to epitaxial Xenes with an interaction with the substrate strong enough to inhibit or minimize the chemisorption to Al adatoms. This usually happens in noble metal surfaces hosting Xene layer as in case of silicene-on-silver and should be further investigated for silicene deposition on sapphire.[21] A question arises as to whether other Xenes of the same kind may benefit from such an encapsulation scheme. More generally, we wonder whether the here reported encapsulation can be taken as a universal methodology for Xenes on metals surface. In the following we give partial response in this respect by taking into account the case of the epitaxial phosphorene.

Encapsulation of epitaxial phosphorene

The strategy developed for the encapsulation of silicene on metallic substrate has been fruitfully exploited to prevent the oxidation of exfoliated black phosphorous flakes on SiO_2/Si substrate.[22] The encapsulation thus works also for highly reactive van der Waals materials on inert substrates. Therefore, it is interesting to further explore its applicability to the vast family of 2D materials with focus on epitaxial Xenes. Epitaxial phosphorene is a good case where to validate the Al_2O_3 encapsulation for metal-supported Xenes beyond silicene-on-silver. Epitaxial phosphorene results from the vacuum evaporation of a P_4 molecular flux that undergoes dissociative chemisorption when grounding on an Au(111) surface. In the substrate temperature range 240-270 °C chemisorbed phosphorus molecular species self-arrange in a flower-like honeycomb pattern with hexagonal symmetry, as shown in the atomically resolved scanning tunneling microscopy (STM) topography of **Figure 4a**. We name this structure epitaxial phosphorene to discriminate it from a single layer of black phosphorus, conventionally termed phosphorene. Differently from silicene, epitaxial phosphorene possesses a local semiconducting character[23,24] and covers completely the whole Au terraces with a single superstructure (**Figure 4b**). The observed morphology has been originally attributed to an epilayer with the same buckled-structure of the theoretically predicted free-standing blue-phosphorene lattice. In this model all the petals of the flower-like pattern corresponds to P_{16} blue-phosphorene islands matching half of the 5x5 Au(111) unit cell.[23–25] However, a close inspection to the high-resolution STM image in **Figure 4a** reveals that only few petals show six bright-protrusions typical of a P_{16} blue-phosphorene island while most of them always consist of three bright protrusions. This has been explained introducing a model where two local atomic configurations may coexist together.[26,27] Beside sparse P_{16} blue-phosphorene islands (see the blue rhombus in **Figure 4a**) also "ad-atom rich" structures are possible. In the "ad-atom rich" structure three additional phosphorus atoms are accommodated on the top layer (see the yellow rhombus in **Figure 4a**). More recently, a new interpretation of the structure of epitaxial-phosphorene questioned all the previously discussed atomic models. As reported in ref.[28] the structure of epitaxial phosphorene may correspond to an Au-decorated phosphorene network rather than to an epilayer. According to this model, the triangular petals coincide with buckled blue-phosphorene P_9 monomers (with the top three P-atoms protruding at a larger distance from the Au substrate) linked to other three P_9 monomers on their sides by gold adatoms coming from the substrate (see the green rhombus in **Figure 4a**).

View Article Online
DOI: 10.1039/C9FD00121B

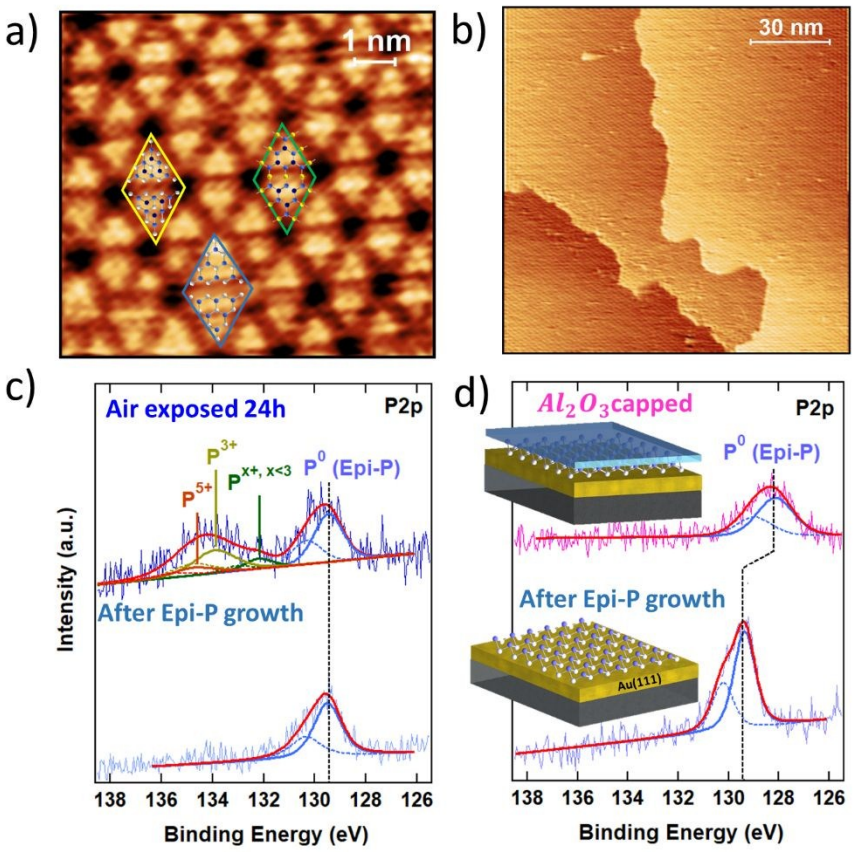

Figure 4 a) High-resolution 8x8 nm^2 STM image of epitaxial phosphorene. The rhombi are (5x5) unit cells enclosing local atomic models proposed for epitaxial-phosphorene: the P_{16} blue-phosphorene structure (blue), the "ad-atom rich" structure (yellow) and the recently proposed Au-decorated Phosphorene network (green). In the overlapping models P-atoms are represented by white, light and dark blue spheres according to the distance from the substrate, Au-atoms by yellow spheres. b) Large-scale 130nmx130 nm^2 STM image of epitaxial-phosphorene c) Comparative XPS study of the P 2p line of freshly grown epitaxial phosphorene (bottom) and after exposure to air (top); d) Comparative XPS study of the P 2p line of freshly grown epitaxial phosphorene (bottom) and after Al_2O_3 encapsulation (top).

Like silicene (but with a different extent), epitaxial phoshorene is subject to oxidation when exposed to air. Its stability is elucidated in the comparative XPS study in **Figure 4c** where the P 2*p* core level photoemission line is reported for freshly grown epitaxial phosphorene (bottom) and after exposure to air (top). As can be noticed from the permanence of the elementary P-P bonding component (denoted P^0 in **Figure 4c**) at 129.4eV epitaxial phosphorene still survives after air exposure in marked contrast with silicene. The photoemitted P 2*p* core electrons of air-exposed epitaxial phosphorene show a broad oxide peak from 132 to 136 eV. By fitting this oxide peak through spin-orbit doublets with a separation of 0.86 eV and a fixed 2:1 intensity ratio, the resulting components at 134.7 eV and 133.8 eV can be attributed to phosphorus oxidation states of +5 and +3 respectively, whereas the component at 132.1 eV can be assigned to lower oxidation states. Thus, the oxidation of epitaxial phosphorene in air may involve the formation of P_2O_5, P_2O_3 oxides and suboxides, $P_2O_{x,\ x<3}$, similar to what has been reported for air-exposed black phosphorus films.[29,30] Oxygen is known to play an important role in the preliminary stages of black phosphorus oxidation,[31] but does not lead alone to a complete physical degradation of the material. Short-term exposures to high-purity O_2 have shown to oxidize few-layer black-phosphorus to a much slower rate than under the combined action of oxygen and water producing low oxidation states.[31] Similarly, epitaxial phosphorene shows a remarkably high oxidation-endurance to limited molecular oxygen dosing in UHV.[26] At higher doses oxygen atoms preferentially absorb on top of one of the protruding phosphorus trimers without degrading the epitaxial phosphorene superstructure.[32] These facts reveal a peculiar oxidation chemistry of epitaxial phosphorene that differs from that of silicene and shares some similarities with the oxidation mechanism of black phosphorus. Accurate investigations are needed to disentangle the oxidation scheme of epitaxial phosphorene and resolve *open questions* such as the chemistry of epitaxial phosphorene with water, alone or in combination with another oxidizing agent like oxygen as well as the influence of the exposure to light.

The effect of the Al_2O_3 encapsulation of the epitaxial phosphorene is elucidated in **Figure 4d** by comparing the P 2*p* line prior to and after Al_2O_3 capping. Despite the reduced photoemission intensity (due to the extra thickness of the Al_2O_3 top layer), the shape profile of the P 2*p* line has no substantial change except for a -1.2 eV shift of the binding energy between the two lines (to a less extent a similar shift is also observed for silicene on Ag). The former fact validates the encapsulating action of the Al_2O_3 layer and candidates Al_2O_3 encapsulation to be a general approach to stabilization of Xenes supported on metal substrates. The latter fact stems from the peak positioning referenced to the Au 4*f* peaks (binding energy positioning of the core level peaks are calibrated on the Au 4*f* position as usual, for each process stage). Shift in the binding energies can be due to charge incorporation causing the Fermi level to move away from its pristine position in the uncapped

layer. We interpret this behaviour as due to an interface dipole formation around the phosphorene environment according to which fixed charges intrinsic in the Al_2O_3 film are compensated by an image charge in the Au/Phosphorene superstructure.[33,34] This picture is corroborated by the observation that the original binding energy is restored whenever the Al_2O_3 capped phosphorene is exposed to air (data not shown) as far as the environmental reactivity may induce the saturation of charged defects in the Al_2O_3 and the reset of the electrical balance between the stacks.

Oxidation of epitaxial phosphorene is a key-aspect to understand in order to develop processing protocols such as transfer or device fabrication. Recently, it was shown that Al_2O_3 encapsulation can save epitaxial phosphorene from complete degradation in a wet environment (used for substrate etching),[26] nonetheless partial oxidation takes place and it is not clear at the moment what is the relevant reactivity path. This is going to *open a framework* where to engineer process enabling the full exploitation of a large-scale phosphorus at the 2D level, thus bypassing size limitation of black phosphorus flakes.

Summary

Xenes are a new frontier for physics and chemistry of 2D materials. However, their stability in environmental condition is a hurdle for applications. This Discussion provides a playground where to deem several aspects of the chemical reactivity of Xenes and to foster a general methodology to face environmental degradation of Xenes out of vacuum. The general character of the Discussion is to propose data inspiring open questions or issues yet to be solved. In detail, the first treated aspect is the chemical reactivity against O_2 exposure and in air. This is showcased in the paradigmatic epitaxial silicene-on-silver by means of photoemission and Raman spectroscopy investigations. Second, a solution to fast degradation of silicene is proposed which consists of the sequential encapsulation of silicene with an Al_2O_3 capping layer. The effectiveness of the approach is substantiated with and supported by a preliminary DFT model suggesting the silicene-silver interaction as key mechanism to save silicene integrity after Al_2O_3 deposition. This idea is further developed on the epitaxial phosphorene-on-gold in order to validate the universality of the approach in the Xene-on-metal framework. In the latter case, the encapsulation works as an effective protection and, due to the peculiar charge exchange at the Al_2O_3 -phosphorene interface, dipole-induced electronic band bending is reported as an effect of the heterostructure. Additional Xenes on metal substrates will represent promising tests to unravel possible universal oxidation mechanisms as well as develop encapsulation processes.

Methods

Samples growth. Epitaxial growth of Xenes was performed in UHV condition (base pressure 10^{-10} mbar) in 210-290 °C temperature range by means of molecular flux released from e-beam evaporators or effusion cells on a metal (Ag, Au) film surfaces supported by a mica substrates and prepared by several cycle of Ar^+ (1 keV) sputtering and annealing at 500 °C. Oxygen dosage experiments were performed in the UHV environment by exposing the silicene surface to O_2-rich atmosphere (100 s and 1000 s at $1x10^{-6}$ mbar to get 75 and 750 L, respectively).

Experimental characterization. Synchrotron radiation core-level photoemission spectroscopy in **Figure 1** was performed at the VUV- beamline at the Elettra Synchrotron Radiation facility in Italy, with the electron spectrometers placed at 45° with respect to the direction of the horizontally polarized photon beam and with a photon energy hv = 130 eV; XPS data in **Figure 2 and 4** are acquired by means of a non-monochromatic Mg Kα source (1253.6 eV) and their energy positioning were calibrated by taking the tabulated Ag and Au core-level positions as references for the case of silicene and phosphorene, respectively; Raman spectroscopy in **Figure 2** with a single 60 s long acquisition by exploiting an Invia Renishaw spectrometer equipped with the 514.5 nm wavelength of an Ar^+ laser Raman spectrum; STM topographies in **Figure 1** and **Figure 4** were acquired at room temperature with an Omicron scanning tunneling microscope (STM) equipped with a homemade chemically etched tungsten tip.

DFT modelling details. *Ab initio* simulations are performed by exploiting DFT with PBE exchange-correlation potential in a generalized gradient approximation (GGA)[35] and using a non-local functional for the van der Waals forces[36] as implemented in Quantum Espresso.[37] We use a plane-wave basis set with a kinetic energy cutoff of 40 Ry and the Γ point for sampling the Brillouin zone of the simulated supercell. The silicene/Ag system has been modeled by a supercell containing 5 Ag(111) atomic layer with the silicene layer on top. The supercell is periodic in the x-y directions, while 15 Å of vacuum has been exploited to avoid interactions between periodic replica in the z direction and a dipole correction has been also used. A single Al atom, an O_2 molecule, or an Al_2O_{12} cluster has been inserted on the silicene surface at an initial distance that ensure the formation of bonds between the Si atoms of the silicene layer and the Al or O atoms on top. Then structural relaxations have been performed until the average atomic force was lower than 10^{-4} Ry/Bohr, by using a quasi-Newton algorithm, both including the Ag substrate and considering a bare free-standing silicene layer

Acknowledgements

The authors acknowledge P. Moras, S. Sanjoy, and C. Carbone (CNR-ISM, Trieste, Italy) for the support in the synchrotron measurements. A.M., C.M. and C.G. acknowledge financial support from funding support from H2020 Framework Programme, call ERC CoG 2017 Grant N. 772261 "XFab".

Conflicts of interest

There are no conflicts to declare.

View Article Online
DOI: 10.1039/C9FD00121B

Notes and references

1 C. Grazianetti, C. Martella and A. Molle, *Phys. status solidi – Rapid Res. Lett.*, 2019, 1900439.

2 A. Molle, J. Goldberger, M. Houssa, Y. Xu, S. C. Zhang and D. Akinwande, *Nat. Mater.*, 2017, 16, 163–169.

3 Y. Xu, B. Yan, H.-J. Zhang, J. Wang, G. Xu, P. Tang, W. Duan and S.-C. Zhang, *Phys. Rev. Lett.*, 2013, **111**, 136804.

4 A. J. Mannix, B. Kiraly, M. C. Hersam and N. P. Guisinger, *Nat. Rev. Chem.*, 2017, **1**, 0014.

5 Y. Yamada-Takamura and R. Friedlein, *Sci. Technol. Adv. Mater.*, 2014, **15**, 064404.

6 A. Molle, C. Grazianetti, L. Tao, D. Taneja, M. H. Alam and D. Akinwande, *Chem. Soc. Rev.*, 2018, **47**, 6370–6387.

7 L. Tao, E. Cinquanta, D. Chiappe, C. Grazianetti, M. Fanciulli, M. Dubey, A. Molle and D. Akinwande, *Nat. Nanotechnol.*, 2015, **10**, 227–231.

8 C. Grazianetti, D. Chiappe, E. Cinquanta, G. Tallarida and M. Fanciulli, *Appl. Surf. Sci.*, 2014, **291**, 109–112.

9 E. Cinquanta, E. Scalise, D. Chiappe, C. Grazianetti and B. Van Den, *J. Phys. Chem. C*, 2013, 1–24.

10 J. Avila, P. De Padova, S. Cho, I. Colambo, S. Lorcy, C. Quaresima, P. Vogt, a. Resta, G. Le Lay and M. C. Asensio, *J. Phys. Condens. Matter*, 2013, **25**, 262001.

11 A. Fleurence, R. Friedlein, T. Ozaki, H. Kawai, Y. Wang and Y. Yamada-Takamura, *Phys. Rev. Lett.*, 2012, **108**, 245501.

12 D. Chiappe, C. Grazianetti, G. Tallarida, M. Fanciulli and A. Molle, *Adv. Mater.*, 2012, **24**, 5088–5093.

13 Y. Du, J. Zhuang, J. Wang, Z. Li, H. Liu, J. Zhao, X. Xu, H. Feng, L. Chen, K. Wu, X. Wang and S. X. Dou, *Sci. Adv.*, 2016, **2**, e1600067–e1600067.

14 C. Büchner, Z.-J. Wang, K. M. Burson, M.-G. Willinger, M. Heyde, R. Schlögl and H.-J. Freund, *ACS Nano*, 2016, **10**, 7982–7989.

15 A. Molle, C. Grazianetti, D. Chiappe, E. Cinquanta, E. Cianci, G. Tallarida and M. Fanciulli, *Adv. Funct. Mater.*, 2013, **23**, 4340–4344.

16 A. C. Ferrari and D. M. Basko, *Nat. Nanotechnol.*, 2013, **8**, 235–246.

17 D. Solonenko, O. D. Gordan, G. Le Lay, H. Şahin, S. Cahangirov, D. R. T. Zahn and P. Vogt, *2D Mater.*, 2016, **4**, 015008.

18 F. L. Galeener, A. J. Leadbetter and M. W. Stringfellow, *Phys. Rev. B*, 1983, **27**, 1052–1078.

19 D. Solonenko, O. Selyshchev, D. R. T. Zahn and P. Vogt, *Phys. status solidi*, 2019, **256**, 1800432.

20 R. Friedlein, H. Van Bui, F. B. Wiggers, Y. Yamada-Takamura, A. Y. Kovalgin and M. P. de Jong, *J. Chem. Phys.*, 2014, **140**, 204705.

21 C. Grazianetti, S. De Rosa, C. Martella, P. Targa, D. Codegoni, P. Gori, O. Pulci, A. Molle and S. Lupi, *Nano Lett.*, 2018, **18**, 7124–7132.

DOI: 10.1039/C9FD00121B

22 J. D. Wood, S. A. Wells, D. Jariwala, K.-S. Chen, E. Cho, V. K. Sangwan, X. Liu, L. J. Lauhon, T. J. Marks and M. C. Hersam, *Nano Lett.*, 2014, **14**, 6964–6970.

23 J. L. Zhang, S. Zhao, C. Han, Z. Wang, S. Zhong, S. Sun, R. Guo, X. Zhou, C. D. Gu, K. Di Yuan, Z. Li and W. Chen, *Nano Lett.*, 2016, **16**, 4903–4908.

24 J. Zhuang, C. Liu, Q. Gao, Y. Liu, H. Feng, X. Xu, J. Wang, J. Zhao, S. X. Dou, Z. Hu and Y. Du, *ACS Nano*, 2018, **12**, 5059–5065.

25 E. Golias, M. Krivenkov, A. Varykhalov, J. Sánchez-Barriga and O. Rader, *Nano Lett.*, 2018, **18**, 6672–6678.

26 C. Grazianetti, G. Faraone, C. Martella, E. Bonera and A. Molle, *Nanoscale*, 2019, **11**, 18232–18237.

27 W. Zhang, H. Enriquez, Y. Tong, A. Bendounan, A. Kara, A. P. Seitsonen, A. J. Mayne, G. Dujardin and H. Oughaddou, *Small*, 2018, **14**, 1804066.

28 H. Tian, J.-Q. Zhang, W. Ho, J.-P. Xu, B. Xia, Y. Xia, J. Fan, H. Xu, M. Xie and S. Y. Tong, *Matter*, , DOI:10.1016/J.MATT.2019.08.001.

29 K. L. Kuntz, R. A. Wells, J. Hu, T. Yang, B. Dong, H. Guo, A. H. Woomer, D. L. Druffel, A. Alabanza, D. Tománek and S. C. Warren, *ACS Appl. Mater. Interfaces*, 2017, **9**, 9126–9135.

30 W. Luo, D. Y. Zemlyanov, C. A. Milligan, Y. Du, L. Yang, Y. Wu and P. D. Ye, *Nanotechnology*, 2016, **27**, 434002.

31 A. Ziletti, A. Carvalho, D. K. Campbell, D. F. Coker and A. H. Castro Neto, *Phys. Rev. Lett.*, 2015, **114**, 046801.

32 J. L. Zhang, S. Zhao, M. Telychko, S. Sun, X. Lian, J. Su, A. Tadich, D. Qi, J. Zhuang, Y. Zheng, Z. Ma, C. Gu, Z. Hu, Y. Du, J. Lu, Z. Li and W. Chen, *Nano Lett.*, 2019, **19**, 5340–5346.

33 L. Kornblum, J. A. Rothschild, Y. Kauffmann, R. Brener and M. Eizenberg, *Phys. Rev. B*, 2011, **84**, 155317.

34 Y. Wu, H.-S. Tao, E. Garfunkel, T. E. Madey and N. D. Shinn, *Surf. Sci.*, 1995, **336**, 123–139.

35 J. P. Perdew, K. Burke and M. Ernzerhof, *Phys. Rev. Lett.*, 1996, **77**, 3865–3868.

36 M. Dion, H. Rydberg, E. Schröder, D. C. Langreth and B. I. Lundqvist, *Phys. Rev. Lett.*, 2004, **92**, 246401.

37 P. Giannozzi, S. Baroni, N. Bonini, M. Calandra, R. Car, C. Cavazzoni, D. Ceresoli, G. L. Chiarotti, M. Cococcioni, I. Dabo, A. Dal Corso, S. de Gironcoli, S. Fabris, G. Fratesi, R. Gebauer, U. Gerstmann, C. Gougoussis, A. Kokalj, M. Lazzeri, L. Martin-Samos, N. Marzari, F. Mauri, R. Mazzarello, S. Paolini, A. Pasquarello, L. Paulatto, C. Sbraccia, S. Scandolo, G. Sclauzero, A. P. Seitsonen, A. Smogunov, P. Umari and R. M. Wentzcovitch, *J. Phys. Condens. Matter*, 2009, **21**, 395502.